Exploiting carbon nanotube networks for damage assessment of fibre reinforced composites

EXPLOITING CARBON NANOTUBE NETWORKS FOR DAMAGE ASSESSMENT OF FIBRE REINFORCED COMPOSITES

A.Baltopoulos[1], N.Polydorides[2], L.Pambaguian[3], A. Vavouliotis[1], V. Kostopoulos[1]*

[1]*Applied Mechanics Laboratory, Mechanical Engineering and Aeronautics Department, University of Patras, Rio - Patras, Greece*

[2] *Institute for Digital Communications, School of Engineering, The University of Edinburgh, Edinburgh, United Kingdom*

[3]*Materials and Components Technology Division, European Space Research and Technology Centre, ESA, Noordwijk, The Netherlands*

ABSTRACT

An approach for damage inspection of composite structures utilizing carbon nanotubes (CNT) networks is investigated. CNT are dispersed in an epoxy using a processing technique compatible with commonly employed composite manufacturing techniques and subsequently used as matrix for a structural glass fiber reinforced composite. The developed electrical conductivity of the composite system is verified experimentally. The electrically conductive CNT network within the GFRP is exploited through distributed electrical voltage measurements to sense and, ultimately, locate damage in the plane of the composite plate. Damage in the form of cracks or delamination interrupts the continuity of the CNT network separating and isolating regions of the conductive network. Employing electric potential fields these changes can become measurable and can provide information for inversely locating the damage. Electrical Resistance Tomography (ERT) is formulated and experimentally applied to measure changes in the potential fields and deliver electrical conductivity change maps which are used to identify and locate changes in the CNT networks. These changes are correlated to capture the damage in the composite. Different damage modes are studied to assess the capabilities of the technique. The technique shows sensitivity to very small damages; less than 0.1% of the inspected area. The solution of the inverse ERT problem delivers a conductivity change maps which offers an effective localization with nearly 10% error and an inspection area suppression of around 75%. The proposed methodology to create CNT networks enables the application of ERT for Non-Destructive Evaluation of composite materials, previously not possible due to lack of conductivity, thus offering damage sensing and location capabilities even in-situ.

Keywords: A. Glass fibres; A. Smart materials; B. Electrical properties; C. Non-destructive testing; Electrical Resistance Tomography

1. Introduction

Damage assessment of composite materials and structures is becoming increasingly important as a consequence of their increased use in a variety of primary importance applications, such as energy and aerospace. Various Non-Destructive Evaluation (NDE) techniques are available to detect damage in

composites with the most commonly employed being ultrasonic (e.g. C-scan) and thermography. The latest years Acoustic Emission, Fiber Bragg Gratings and use of vibration-based methods have attracted a great amount of attention. In parallel, the progress in nanotechnology has enabled the development of novel materials routes for developing multi-functional material systems that incorporate approaches for damage detection.

Products of nanotechnology, such as Carbon Nanotubes (CNT), Carbon Black (CB) or other nano-particles, have been proposed as additives for mechanical performance enhancement of composites through their incorporation in the matrix [1]. Promising results have been reported in fatigue, fracture and post impact performance of such systems [2]. In parallel to the mechanical performance, the integrated nano-particle networks within polymer matrices can be employed for damage sensing and monitoring of the composites performance. This added functionality enables a multifunctional performance of composites. Most of the reported works in this direction are based on the Electrical Resistance Change Method (ERCM) where the apparent macroscopic resistance of the conductive network is monitored. Relation has been proven between the recorded electrical resistance change and the loading incidents and/or the mechanical degradation of the material. Studies have covered a wide spectrum of materials; nanocomposite polymers [3] and polymer foams [4], Glass Fibre Reinforced Plastics (GFRP) [5-8], Carbon Fibre Reinforced Plastics (CFRP) [9]. Finite Element (FE) models have also been employed to verify the experimental findings [10]. It can be said that electrical-based methods, such as ERCM, offer the potential of a tool for sensing the development and evolution of damage as well as health monitoring of conductive composite structures.

In order, however, for both nano-particle networks and electrical based methods to reach real applications at large scale, further developments are needed; developments to extend the capabilities in the localization of the damage and the estimation of its size based on the needs of practice. A number of studies have worked in extending electrical sensing principles to 2D using electrical conductivity mapping [11], electric potential fields [12] or other approaches [13]. A brief summary of the ideas is presented in [14].

Some works have been reported in the recent in the direction of exploiting nano-particle networks in structural composites to provide 2D inspection information. Hou et al [15] employed a tomographic approach to demonstrate multifunctionality of a specially prepared CNT-based film. The system was used as a sensing element on the surface of a structure and was able to detect impact incidents. Ye et al [16] used dispersed CB and copper chloride nano-particles in Glass/Epoxy composites

for enabling electrical damage sensing. They proposed a tomographic approach and used the change of electrical resistance as a damage index. An intuitive probabilistic formulation was employed, where the cumulative contribution of individual sensing paths is considered for delivering damage assessment maps. The technique performed well in assessing and quantifying impact induced damage. Proper et al [17] developed a Multi Wall CNT (MWCNT) network into a Kevlar composite. Following, an external electrode grid was attached on the surface of the plate to sense the potential distribution. They were able to point to the location of the impact damage by comparing the patterns before and after impact damage and relating the grid potentials to the conductivity distribution within the composite. Loyola et al. [18] demonstrated the performance of Electrical Impedance Tomography (EIT) as an embedded Structural Health Monitoring (SHM) methodology, where following a purpose-specific process a conductive and strain-sensitive film was deposited within the electrically non-conductive GFRP structure. The actively sensing region partly covered the GFRP part, was 80x80 mm in dimensions and employed 32 peripheral electrodes. An intuitive current pattern definition was employed being adjusted for the anisotropic electrical properties of the sensing region. The results indicated that EIT can detect and locate different modes of damage with good sensitivity. Alternative routes based on nanotechnology and multi-physics fields have also been proposed by Guzman de Villoria et al [19] enabling good spatial resolution for sensing damage in composites. Viets et al. [20] demonstrated damage mapping of carbon nano-particles modified GFRP via electrical resistance measurements. They dispersed MWCNT at 0.3%wt. and 0.7%wt and CB at 12%wt in the matrix of GFRP via three-roll mill mixing. Following, they deployed a series of silver ink strip electrodes over the surface of a composite part; 10 per side with the two sides being perpendicular. They used out-of-plane resistance measurements occurring from pairs of opposite-side electrodes to monitor the damage developed by impact. It was shown that the detection and localisation of barely visible impact-related damages via electrical resistance measurements was possible with the developed technique. The significant influence of the different nanoparticles and filler contents on the results of the damage mapping, especially regarding the sensitivity of the resistance to damage, was shown. More recently, Tallman et al. [21] used CB for enabling electrical monitoring of GFRP composites. They established a preferential aligned arrangement of the CB particles and determined the sensitivity of the EIT to through-hole damage as well as the ability of the technique to capture impact and multiple damage sites. They demonstrated the considerable potential of conductivity-based health monitoring for glass fiber reinforced polymer laminates with conductive networks of nanoparticles in the matrix.

In the present work, a methodology is presented to develop a 3D CNT network in the matrix of a fibre reinforced composite, which is subsequently exploited to sense damage and through a proposed tomographic technique to provide information of the location of the damage. For developing the CNT network, a processing technique compatible with conventional composite manufacturing technologies is utilized. The sensing scheme takes a step further from the state-of-the-art in sensing studies utilizing CNT networks by providing a structured methodology to calculate inspection maps for locating damage in composite parts. Electrical Resistance Tomography (ERT) [11, 22] protocol is used for collecting and processing the experimental recordings, transferring technology and experience from other scientific fields [23, 24]. The outcome of this ERT inverse problem solution is a map of the expected electrical conductivity changes, corresponding to the part under inspection. From this map, one can identify regions of interest (e.g. high change in conductivity) and such a technique can serve as a tool for the NDE of composite parts. It is believed that the proposed approach is scalable and can serve as the basis for further applications of CNT networks in real structures.

This work expands the state-of-the-art by presenting a case study which synergizes nanotechnology for composites and superior NDE techniques. It builds upon existing experience [25, 26] and formalizes the NDE methodology, bridging the field between the research by Proper et al [17], Hou et al [15], Viets et al [20] and Tallman et al [21] in terms of combination of materials (MWCNT) and electrical sensing application (i.e. electrode design and positioning, post-processing framework).

Both the material preparation process and NDE methodologies proposed are extendable to other nano-particle as long as the amount of nano-particles in the matrix is above the percolation threshold to reach a conductive network throughout the composite. In this sense, a critical advantage of the CNT exists as the percolation can be reached much lower in weight percentage and, consequently, the processing of the epoxy is less affected and the mechanical properties of the composites are not sacrificed.

2. Principle idea of the work

The CNT reinforced GFRP essentially represents a three-phase composite system comprising the matrix, the CNT network and the glass fibers. Both the glass fibers and the matrix are insulating phases. The only path for electrical charge transport in the composite is the conductive CNT network. The network extends throughout the matrix of the composite providing an efficient path for electron flow, similar to a distributed network of resistors [27]. The conductivity of the composite system is leveraged for NDE. The

principle idea of this work is illustrated in a simplified way in the schematic of Figure 1. For clarity, glass fibers are excluded from the schematic.

In practice, the tools in hand are a current source and a voltage meter. Injecting a current at different points of the CNT network stimulates different regions of the network and develops a different voltage distribution throughout the material. Thus, as it seems natural, when monitoring the voltage at the same end of the network a different voltage value will be recorded (Figure 1-a, b). Maximizing the sensitivity of the voltage measurement by adjusting the current injection point seems like a logical approach.

When damage is considered, any defect in the CNT network (e.g. due to cracking or delamination) will create a local disruption in the electrical network (Figure 1-c, d). Parts of the network may be separated and isolated and this will have an effect on the total apparent resistance (seen by the current source) and the local current flow (seen at the voltage measurement ends). This means that when injecting a current at the same location to the network, a different electrical potential field will be established between the undamaged and the damaged state. Taking a step further, by injecting current at different points of the network, the effect of the disturbance on the boundary voltage measurements may be magnified or suppressed.

These two observations form the basis of the proposed tomographic technique. Based on a vector of electrical potential information measured at the boundary of the composite laminate, we attempt to inversely calculate the conductivity distribution change within the material. Because the CNT are considered homogeneously distributed within the matrix in a 3D configuration, this enables a global monitoring of the composite laminate and can address various related damage modes.

3. Materials, Methods and Experimental Approach

3.1. Preparation of CNT-polymer mixture and manufacturing of the composite material

Epoxy resin L1100 (with Hardener 295) commercially available by R&G Composite Technologies GmbH (Germany) was used as the host matrix. It is a low viscosity resin system, widely used in wind turbine blade manufacturing. The macro-scale reinforcing phase was a glass fiber twill woven fabric having a 163gr/m^2 area weight, procured by R&G Composite Technologies GmbH (Germany). MWCNT produced by catalyzed Chemical Vapor Deposition (CVD) were supplied by ARKEMA (France) in raw powder form. The MWCNT had a diameter ranging from 10 to 15nm and length reaching up to 750nm, resulting in an aspect ratio between 30 and 50. The MWCNT were used as received, i.e. no treatment or

functionalization took place. Any humidity present was removed by placing the CNT in an oven at 60°C for 12hrs prior to the mixing process.

The dispersion and composite manufacturing procedure is shown in Figure 2. The first step is to disperse the MWCNT in the bisphenol-A (Part-A of the epoxy system) (Step 1). High-shear mixing dissolver device by VMA Getzmann GmbH (Germany) was used to homogeneously disperse the CNT. The targeted CNT concentration in the final composite was 0.5%wt. The required amounts are weighted and added into the same container. A rotating disk introduces shear forces to the mixture creating a vortex flow (known as the "doughnut effect") which leads to a continuous mixing of the compound. The shear forces disentangle the CNT and reduce their agglomerates. The dissolver disc rotational speed was 2500rpm and the mixing duration was 3hrs. The temperature was controlled between 40-50°C using a water cooled double walled container. The mixing was performed under vacuum to avoid any air inclusion in the mixture and consequently in the composite. The technique has proven to be effective in dispersing CNT in epoxy systems in order to produce electrically conductive composites, utilizing efficiently the advantage of high aspect ratio of the CNT [28].

Then the amine hardener was added (Step 2) and subsequently the nano-reinforced resin was used to fabricate glass fiber composites (Step 3). Prior to layup the resin was degassed for 15min. Twelve (12) layers having the same orientation were used. Layer by layer wet-layup was used. The lay-up took place on a rigid flat aluminum mould. Once the wet lay-up process was finished, the stack was hermetically enclosed in a vacuum bag, vacuumed and put in an oven to cure for 6hrs at 50°C. The produced plate had dimensions 300x300 mm and thickness of 2.5mm. The resulting fibre volume fraction of the composite was determined to be 47%±2.

For the ERT campaign, square 100mm specimens were cut from the plate using a diamond-grit circular disk. The specimens were prepared for ERT by positioning 20 peripheral electrodes close to the edge of the plate. Firstly, a 1mm diameter hole is drilled at the desired point. The inner surface of the hole is painted with conductive silver-paint to provide a good interface and minimize contact resistance with the circular cross section copper electrode, which is placed tightly into the hole. A two part conductive epoxy (CircuitWorks® Conductive Epoxy by Chemtronics), commonly used for solderless electronic connections, is used to hold the electrode cables in place while allowing electrical conduction (similar to [15, 22]). The epoxy was cured for 4hrs at 55°C.

3.2. Material Characterization

To evaluate the dispersion of CNT within the matrix Scanning Electron Micrographs (SEM) and electrical conductivity measurements were used. Images were taken using LEO SUPRA 35VP at various magnification levels for a set of random samples from the material.

A KEITHLEY 2002 digital multimeter by Keithley Instruments Inc. (USA) was used for the electrical measurements. Measurements were made in three directions corresponding to the three principle axes of the material. Specimens were cut from the manufactured plate; oblong specimens 100x15mm for in-plane measurements (X-axis and Y-axis) [29] and square 25x25mm specimens for the through thickness direction (Z-axis). Al least five (5) specimens were measured for each direction. The electrode contact surfaces were sanded to smooth the roughness from the peel ply and then silver painted twice to create a uniform and smooth coating using commercially available conductive silver paint (RS Components Silver Paint Conductive Adhesive).

3.3. Damage modes assessed

To assess the sensing capabilities of ERT on these materials, three different damage scenarios were evaluated (Figure 3); a through-thickness hole, an oblong notch and indentation damage.

The through hole (Figure 3-a) is the first damage implemented to assess the capabilities of NDE/SHM methods. It is used to assess baseline sensitivity of the technique. Here a small hole having a diameter of 3mm was made to the plate. The damage corresponds to less than 0.1% of the total area of the composite plate being inspected.

An oblong notch (Figure 3-b) is another typical damage mode assessed in NDE/SHM works and is an approach to assess the capability of the technique to detect cracks. An oblong crack was created using a cutting disc and a high speed rotary tool (DREMEL). The damage region represented nearly 0.2% of the total inspected area.

Finally, Quasi-Static Indentation (QSI) was employed to experimentally assess the proposed approach as a step towards Barely Visible Impact Damage (BVID) detection. BVID is a major concern in structural composite parts as it is the result of accidental low energy impact event and can severely degrade the mechanical performance of the part. In QSI test (Figure 3-c), a hemispherical indenter (Φ 12mm) is pushed against a simply supported specimen. The support is a circular ring (50mm diameter) leaving the space under the specimen, right below the indentation point free to deform. The loading continues until a drop in the force is recorded. Then the test is stopped, the specimen is unloaded and inspected. To assess the developed damage (Figure 3-d) and for direct evaluation of the ERT results, ultrasonic inspection (C-scan) was employed.

3.4. ERT theory, post-processing and application

The forward electrical problem is to derive the voltage distribution given the conductivity distribution within a medium and the current injection input. Mathematically this is done by solving Equation 1 in the conductive medium Ω, given appropriate boundary conditions:

$$\nabla \cdot (\sigma \nabla u) = 0 \ , \qquad \bar{r} \in \Omega \tag{1}$$

Where σ is the conductivity distribution and u is the electrostatic potential.

The Electrical Tomography Inverse Problem (ETIP) is the process of approximating the conductivity distribution in the interior of a body from the knowledge of currents injected in the medium and voltages measured at its surface. The result of the ETIP is a conductivity change map corresponding to the volume under inspection.

A series of electrodes is placed at the periphery of the part under inspection (Figure 4-a). Current is injected through a selected set of two electrodes (corresponding to the ground and the Vcc-positive supply voltage). Voltage measurements are recorded on the rest of the electrodes. The process is organized in a protocol which defines which electrodes are active (current bearing) and which are passive (voltage sensing). The recorded measurements along with the geometry of the component and electrode location are used as input for the inverse calculation of the conductivity change distribution. Certain sets of electrodes for current injection may prove more informative, based on the type, the location and the extent of damage. However, since the damage characteristics are unknown, there is no a-priori knowledge.

ETIP is an ill-posed problem and intrinsically non-linear which means that small variations in the input (voltage measurements) may have large effects on the output (conductivity maps). This nature of inverse ERT problems sets limitations to the capabilities of the technique. It is not within the scope or the capacity of this work to cover all the details regarding ill-posed problems and techniques to address this issue. Nevertheless, interested readers are encouraged to read further in [23, 30]. Here we address issues relevant to the presented application of the ERT technique to exploit CNT networks for damage detection and assessment.

To deal with the ill-posedness of the inverse problem, we employ a post-processing scheme recently proven to perform well in materials of similar nature [22]. The mathematical inversion of the experimental data to calculate the conductivity change map is performed following the Tikhonov regularization (Equation 2) [24]:

$$d\sigma_{Tikhonov} = \min\{\|dV - J(d\sigma)\|^2 + \lambda\|L \cdot d\sigma\|^2\} \quad (2)$$

Where: $d\sigma_{(Tikhonov)}$ is the conductivity change vector, dV is the experimentally recorded voltage change between two states, J is the Jacobian mapping the conductivity change to voltage change on the electrodes, λ is the regularization parameter and L is the regularization matrix. Essentially, it is a Least Squares approach augmented by an additional penalty to large solutions. Regularization improves the conditioning of the problem, enabling a numerical solution. The identity matrix was used as L to avoid any bias to the solution, while a heuristic approach was followed to select the value of λ.

For the solution of Equation 2, an FE scheme is employed in the mathematical formulation of the inverse problem [30, 31]. The conductivity is kept constant within each element of the FE mesh, while the voltage was piecewise linear. The process essentially assigns a conductivity change value to each element of the mesh to reach a best fit solution of J(dσ) to dV which is governed by the Jacobian of the inverse problem (J). The outcome is an electrical conductivity change map depicting where changes are expected between the two states compared; an increase in the conductivity change map is essentially a region where conductivity is expected to drop.

As a step to further automate the damage assessment and to enhance the localization of the technique, two indices are calculated for each calculated map; the Centre of Interest (CoI) and the respective Region of Interests (RoI). The former refers to the mathematical areal weighted mean of the conductivity change distribution while the later is the 1-σ region around the CoI. Both the CoI and the RoI have the scope to provide a point location of the interest to limit the inspection region and concentrate the interest based on the calculated map. Details on the calculation can be found in [22] and references therein.

For implementing experimentally the technique, an ERT system was developed. A conceptual illustration of the ERT system and the process as applied in this work is shown in Figure 4-a. The experimental setup used in this work is shown in Figure 4-b. The ERT system consists of a programmable DC source (KEITHLEY 224) and a data acquisition switch board unit with an internal digital multi-meter (AGILENT 34970A). Dedicated routines control the switching within the cards of the data acquisition unit to deliver the current at the desired electrodes and take the voltage measurements according to a specified protocol.

The opposite current injection protocol [30] for collecting the voltages is used. The protocol runs as follows. Current is injected between the first pair of electrodes (electrodes 1 & electrode 11: current pattern 1-11). A sub-set of voltage measurements is taken for all the electrodes with reference to the

ground (V@1,2,3,...,20). Then, the next current pattern is applied at the next opposite electrode pair (current pattern 2-12). Again the system is allowed to settle and the respective sub-set of voltage measurements (V@1,...,20) is recorded. This loop is continued for current patterns up to 10-20 where the process is ended. A total of 10 current patterns is used. For each current pattern 20 measurements are available. This results in signature with a global set of 200 measurements.

For assessing each damage, a signature set is taken prior to damage as reference and another signature set is recorded after the damage is introduced. Their difference is the input (dV) for Equation 2.

4. Results and Discussions

4.1. Properties of the composite and observation of the percolated CNT network

Figure 5 shows a series of SEM pictures at different magnifications. A large number of images was captured at random locations of the composite to verify the homogeneous dispersion of CNT. In Figure 5-a, a macroscopic image of the fracture surface of the composite is seen where the imprints of detached fibers are evident. The fractured surface of the resin reveals the internal distribution of the CNT. A close view of the fracture surface and the fiber-matrix interface is seen In Figure 5–b, c. Individual and clustered CNT are evidently spread in the matrix and are identifiable by their white color in contrast to the darker area of the pure resin. Agglomerated CNT are indicated by ellipses. A better dispersion is evident in Figure 5-c, where a whole region of the resin is covered by randomly dispersed CNT. CNT are present in the inter-fiber region indicating a good infiltration within the layers of glass fibers. Figure 5-d shows a close up of an agglomerate broken at the surface and CNT protruding from the matrix in a random fashion. The SEM micrographs indicate a high degree of dispersion of the CNT despite the fact that agglomerates are present. This observation in turn gives rise to the presence of a percolated CNT network throughout the composite.

To further verify the percolation of CNT network within the composite, the electrical conductivity of the material in the X, Y and Z directions was experimentally derived. The obtained values were: $\sigma_X = 6.02 \pm 0.44 \cdot 10^{-3}$ S/m, $\sigma_Y = 6.61 \pm 0.48 \cdot 10^{-3}$ S/m and $\sigma_Z = 1.54 \pm 0.53 \cdot 10^{-4}$ S/m. It is seen that the conductivity in the X-Y plane is essentially the same while the value for the Z direction is relatively lower. The difference is not considered significant as all conductivity values achieved fall at the same range as in the works of [3, 8, 32]. Achieving a perfectly dispersed system of CNT is extremely difficult and the intermediate processing steps (layup, curing etc.) play their role in not supporting this.

Nevertheless matter-of-factly, this may not be an issue as the achieved 3D network of CNT provides conductive pathways adequate for sensing load, strain and damage [3, 8].

4.2. Sensing Baseline Damage and Cracks

A very small current ($I = 10^{-5}A$) was required to reach a signal-to-noise ratio over 50dB for the voltage measurements. The selection of the current was done based on practical aspects of the setup and the composite such as the resistance of the sample (in the range of kΩ), the maximum voltage of the power supply and a readable voltage level on the peripheral electrodes. This current can produce significant and measurable voltages to enable the detection of changes and, as will be shown later, it was sufficient to distinguish changes between the reference and the damaged state. In previous studies on CFRP the required current was 0.1A [22], an observation that reflects the role of material conductivity in the application of ERT.

The first damage case was used for the baseline evaluation of the approach. A through thickness hole was drilled at $(X_{hole},Y_{hole}) = (38.0, 23.4)$mm. The damaged specimen is seen in Figure 6-a. Using the recorded values, a conductivity change map is calculated and shown in Figure 6-b. The map shows a smooth baseline in the largest portion of the inspected area. According to the inverse calculation, conductivity change is expected at the central bottom region of the part; close to electrodes 13 and 14. A dipole-like field is predicted close to electrode 13, having similarities to the observations by Proper et al [17], where a distributed mesh of sensors was used. No other region presents specific peaks or other interesting features for further evaluation. From the automated process, the CoI was calculated to be at $(X_{COI\text{-}hole},Y_{COI\text{-}hole}) = (45.9, 30.7)$mm. The respective RoI represents a 16.9% of the total inspected area. Evidently, the hole falls within the identified RoI. Considering the distance between the real location, the estimated CoI and the size of the inspected area, the localization error is nearly 10% for exactly locating the point of damage. Given this, it can be said that the proposed synergistic NDE approach performs satisfactorily capturing the damage with marginal error.

The second damage mode that was assessed was an oblong notch. The notch was created having a -30^{o} angle to the horizontal. The centre of the notch was at $(X_{notch},Y_{notch}) = (63.0, 70.5)$mm. The thickness of the notch was 2mm while the length of the notch was 16mm. The damaged specimen is seen in Figure 7-a. The inserted photograph shows the zoomed region of the notch. The conductivity change map calculated for this damage mode is shown in Figure 7-b. The map is smooth throughout the central region of the inspected area, indicating no changes. An extended region of conductivity change is predicted at the central top region of the part close to electrodes 3 and 4. The CoI for the case of the notch

is located at ($X_{COI\text{-}notch}$,$Y_{COI\text{-}notch}$) = (57.2, 60.0)mm. The RoI represents 22.1% of the total inspected area. Despite the fact that a clear oblong shape change that would directly reflect the notch is not revealed, the notch falls within the identified RoI and close to the CoI with a localization error of nearly 12%.

As seen from the reconstructed maps, the solution suffers limited resolution away from the electrodes. This is well known in ERT and is due to the ill-posed nature of the problem and the exponential decay of the electric field. In the studied case, this is expressed by low resolution and limited diffusion of the solution in the central region of the part.

To increase the sensitivity in the central region of such parts, (a) the optimization of the injection pattern for given expected damage mode and (b) increasing the number of peripheral electrodes with respect to the dimensions of the inspected part could be considered.

On the one hand, current injection strategies could be alternatively selected so as to deliver higher current densities close to the damaged region and thus improve the sensitivity of the technique [33].

On the other hand, increasing the number of electrodes on the periphery of the part may be useful as a means to increase the available information of the developed potential field. This is seen in the study by Hou et al [15] where a series of 32 electrodes was used for films of much smaller dimensions (~25mm). The results provided are impressively more informative and straightforward for evaluation. It is believed that it is the relation of size and number of electrodes that provides this enhanced sensitivity. Having more data as input can provide better indications, even though there is a certain limit after which more data does not necessarily mean better maps. It is the independent data that is needed to increase the reconstruction resolution.

Alternative approaches have been employed by Angelidis et al. [12], Proper et al. [17], Naghashpour et al. [34], Viets et al. [20] who did not constrain the placement of the electrodes only at the edges of the part. Grids of point electrodes on the surfaces of the part or strips extending over the whole length of the part were used as electrodes. The results indicated a very high sensitivity of the approaches, without considering the integration penalty of these methods (e.g. scale-up, invasiveness, cabling). Taking into consideration the scaling perspective of all the approaches and the requirements of structural cases for low mass and minimal invasion, another optimization problem is formulated where the number of electrodes in a given allowable region needs to be minimized over a sensible and informative inspection map. Thus the trade-off between the sensitivity and the electrodes needs to be considered for

each case studied. It is believed that the presented ERT scheme complements the works in literature and delivers highly informative maps at a minimal integration penalty.

4.3. Barely Visible Impact Damage

BVID is commonly expressed as interlaminar damage which has not propagated to the outer layers of the composite and thus is not distinguishable to the naked eye. NDE techniques are suitable to assess such damage. Indentation is employed here to simulate BVID. Figure 8-a shows a snapshot of the indentation experiment. The indentation point was at an off-centre position (X_{BVID}, Y_{BVID}) = (55.0, 27.5)mm. The corresponding force-displacement curve recorded is shown in Figure 8-b. The experiment was terminated when a drop of the load was recorded which indicated the loss of load bearing capability. The specimen after the indentation is shown in Figure 8-c. The visual inspection revealed a permanent imprint on the indentation side and the debonding of some fiber bundles on the back of the specimen. The corresponding C-scan inspection map is shown in Figure 8-d. According to the benchmark technique, a concentrated change in thickness at the indentation point is revealed as a darker circular region, corresponding to the imprint of the indenter. The local debonding of the bundles just below the indentation point is revealed as dark lines extending in the Y-axis up till after the middle of the specimen. The C-scan shows that the delamination has not propagated in the XY plane. The rest of the part remained intact.

The debonded bundles are impregnated with the resin and thus carry CNT. The fact that the bundles have been detached means that the conductive network at the region has been disrupted and the CNT network around the fibers has been disconnected. Locally, resistance will be larger as the cross-section decreases and this is expected to be reflected on the electrical measurements close to the neighboring electrodes.

The experimental voltage recordings before and after the indentation were used to calculate the conductivity change map which is shown in Figure 8-e. The main interesting section of the conductivity change map is at the central bottom region of the part. An oblong strip of conductivity change is predicted between electrodes 12 and 13 extending up to 1/3 of the plate's Y-dimension. This region corresponds precisely to the real location of the imprint and the fiber bundle debonding. The rest of the map is relatively smooth throughout the central region of the inspected area and some minor pair-wise changes are predicted at the periphery of the part (top and left side).

The CoI for the case of the notch is located at ($X_{COI\text{-}BVID}$, $Y_{COI\text{-}BVID}$) = (51.3, 47.6)mm. The RoI represents a 25.1% of the total inspected area. Due to the extended dimensions of the real damage, the damage localization error in this case is relatively larger (nearly 18%) than in the other cases.

Nevertheless, the largest part of the damaged region, including the indentation point, falls within the identified RoI. Furthermore, the conductivity change region identified correlates with the imprint and the debonding area.

5. Conclusions

The formation of CNT networks within the matrix of an insulating composite has been shown to offer a new functionality to the structural material, i.e. electrical, which is leveraged for NDE. The major conclusions of the work are summarized here:

(1) Polymer processing and mixing techniques compatible with widely used composite manufacturing techniques are employed to develop the CNT network within the matrix of the composite.

(2) The electrical conductivity of the composite system occurring due to the CNT network has been measured and exhibits isotropic in-plane conductivity which is higher than the out-of-plane conductivity of the composite.

(3) An approach based on ERT has been proposed and studied to exploit the created CNT networks within the matrix of the composites for NDE. A structured ERT methodology is presented and applied on CNT reinforced GFRP. Parameters for further adaption and customization of the methodology by interested researchers are also discussed.

(4) Electric potential methods for sensing damage in CNT networks have proven to be sensitive to very small changes in the network, even as small as 0.1% of the total inspected area. It is possible to detect different types of damage that disrupt the structure of the CNT network and are relevant to composites. The changes induces in the field by the damage are measureable at the edges of the composite and convey sufficient information for solving the ETIP.

(5) It is possible to calculate meaningful ETIP solutions based on the proposed formulation. The calculated electrical conductivity change maps of the structure convey meaningful information and can serve well as inspection maps to direct to the location of the damage as they capture the changes and directly correspond to the composite part under inspection.

(6) The calculated features (i.e. CoI and RoI) performed well in indicating the position of the real damage and successfully predicted the region of it. The inspection area in all the cases was suppressed, reaching up to 83% decrease, which can be translated to fast inspection cycles.

In general, very low currents were sufficient to invoke detectable voltage changes at the boundaries of the CNT network within the laminate. The power requirement for this technique is much less than 1W and

currents are very small to involve any risk. Alternative ERT strategies (e.g. injection patterns) are feasible and the methodology is customizable to the respective application (e.g. different geometries). The fact that the calculation scheme is fully compatible with FE gives potential for integration of the technique in more complex systems. Developing cross-property relations for such materials (e.g. strength relation to electrical conductivity) could enable translation of conductivity change maps to strength degradation and lead to structural failure prognosis within FEA formulations.

Acknowledgements

Part of this work has been funded by the European Commission EU-FP7-AAT project IAPETUS (Grant Agreement Number: ACP8-GA-2009-234333). Athanasios Baltopoulos would like to acknowledge the support from the Greek State Scholarship Foundation (IKY), the Greek General Secretariat of Research and Technology and the European Space Agency – Greek Task Force through the ESA Greek Trainee Program. The authors would like to thank Michele Muschitiello and Andrew Norman of ESA/ESTEC for their support and ideas on the development of ERT and the experimental setup, respectively.

References

[1] Qiu J, Zhang C, Wang B, Liang R. Carbon nanotube integrated multifunctional multiscale composites. Nanotechnology 2007;18:275708.

[2] Youhong Tang, Lin Ye, Zhong Zhang, Klaus Friedrich. Interlaminar fracture toughness and CAI strength of fibre-reinforced composites with nanoparticles – A review. Composites Science and Technology 86 (2013) 26–37

[3] F.H. Gojny, M.H.G. Wichmann, B. Fiedler, W. Bauhofer, K. Schulte, Influence of nano-modification on the mechanical and electrical properties of conventional fibre-reinforced composites. Composites A 36 (2005) pp.1525-1535.

[4] Baltopoulos A, Athanasopoulos N, Fotiou I, Vavouliotis A, Kostopoulos V. Sensing strain and damage in polyurethane/MWCNT nano-composite foams using electrical measurements. eXPRESS Polymer Letters 2013;7(1):40–54.

[5] Thostenson E, Chou T-W. Carbon Nanotube Networks: Sensing of Distributed Strain and Damage for Life Prediction and Self Healing. Adv. Mater. 2006;18:2837–2841.

[6] Sotiriadis G, Tsotra P, Paipetis A, Kostopoulos V. Stiffness degradation monitoring of carbon nanotube doped glass/vinylester composites via resistance measurements. J Nanostructured Polymers and Nanocomposites 2007;3(03):90-95

[7] Gao L, Chou T-W, Thostenson E, Zhang Z, Coulaud M. In situ sensing of impact damage in epoxy/glass fiber composites using percolating carbon nanotube networks. Carbon 2011;49:3371–3391.

[8] Nofar M., Hoa S.V, Pugh M.D. Failure detection and monitoring in polymer matrix composites subjected to static and dynamic loads using carbon nanotube networks. Comp Sci Technol 2009;69:1599–1606.

[9] Vavouliotis, A., Paipetis, A., Kostopoulos, V. On the fatigue life prediction of CFRP laminates using the Electrical Resistance Change method. Comp Sci Technol 2011;71(5):630-642.

[10] Li C, Chou T-W. Modeling of damage sensing in fiber composites using carbon nanotube networks. Comp Sci Technol 2008;68:3373–3379.

[11] Schueler R, Joshi SP, Schulte K. Damage detection in CFRP by electrical conductivity mapping. Compos Sci Technol 2001;61:921–30.

[12] Angelidis N, Irving P.E. Detection of impact damage in CFRP laminates by means of electrical potential techniques. Comp Sci Technol 2007;67:594–604.

[13] Takahashi K, Hahn T. Towards practical application of electrical resistance change measurement for damage monitoring using an addressable conducting network. Structural Health Monitoring 2012;11(3):367–377.

[14] Wang D, Wang S, Chung D.D.L, Chung J. Sensitivity of the two-dimensional electric potential/resistance method for damage monitoring in carbon fiber polymer-matrix composite. J Mater Sci 2006; 41:4839–4846.

[15] Hou T-C, Loh KJ, Lynch JP. Spatial conductivity mapping of carbon nanotube composite thin films by electrical impedance tomography for sensing applications. Nanotechnology 2007;18:315501.

[16] Ye L, Zhang D, Wang D. Interlaminar fracture and impact damage assessment by electrical resistivity tomography in GFRP laminates with conductive nanoparticles. Proceedings of the 15th European Conference on Composite Materials, Venice, Italy, 24-28 June 2012.

[17] Proper A, Zhang W, Bartolucci S, Oberai A, Koratkar N. In-Situ Detection of Impact Damage in Composites Using Carbon Nanotube Sensor Networks. Nanoscience and Nanotechnology Letters 2009;1: 3–7.

[18] Loyola B. R. et al., "Detection of Spatially Distributed Damage in Fiber-Reinforced Polymer Composites", 2013, Structural Health Monitoring, 12, pp. 225-239, doi: 10.1177/1475921713479642

[19] Guzman de Villoria R, Yamamoto N, Miravete A, Wardle B. Multi-physics damage sensing in nano-engineered structural composites. Nanotechnology 2011;22:185502.

[20] Christian Viets, Simon Kaysser, Karl Schulte. Damage mapping of GFRP via electrical resistance measurements using nanocomposite epoxy matrix systems. Composites Part B: Engineering Volume 65, October 2014, Pages 80–88

[21] Tyler N Tallman, Sila Gungor, K W Wang, Charles E Bakis, Damage detection via electrical impedance tomography in glass fiber/epoxy laminates with carbon black filler. published online before print October 16, 2014, doi: 10.1177/1475921714554142

[22] Baltopoulos A, Polydorides N, Pambaguian L, Vavouliotis A, Kostopoulos V. Damage identification in CFRP plates using electrical resistance tomography mapping. J Comp Mater, DOI: 10.1177/0021998312464079.

[23] Lionheart W, Polydorides N, Borsic A. The reconstruction problem, in "Electrical Impedance Tomography: Methods, History and Applications", edited by D. Holder, IOP Publishing, Bristol, 2005:3-64.

[24] Vauhkonen M, Vadasz D, Karjalainen P, Somersalo E, Kaipio J. Tikhonov Regularization and Prior Information in Electrical Impedance Tomography, IEEE Trans Med Imag 1998;17(2):285-293.

[25] A. Baltopoulos, N. Polydorides, A. Vavouliotis, V. Kostopoulos, L. Pambaguian. Sensing capabilities of multifunctional composite materials using carbon Nanotubes. 61st International Astronautical Congress, IAC 2010, Prague, Czech Republic, 11004-11012.

[26] Baltopoulos A., Polydorides N., Pambaguian L., Vavouliotis A., Kostopoulos V. Electrical tomography as a tool for non-destructive assessment of composite structures, in "Emerging Technologies in Non-Destructive Testing V", Edited by Paipetis A., Van Hemelrijck D., Aggelis D. and Matikas T. Taylor & Francis Group, London, pp. 389- 394. (2012).

[27] Lazarovitch R, Rittel D, Bucher I. Experimental crack identification using electrical impedance tomography. NDT&E International 2002;35:301-316.

[28] Vavouliotis A, Fiamegou E, Karapappas P, Psarras GC, Kostopoulos V. DC and AC conductivity in epoxy resin/multiwall carbon nanotubes percolative system. Polymer Composites 2010;31:1874–1880.

[29] N. Athanasopoulos, V. Kostopoulos. Prediction and experimental validation of the electrical conductivity of dry carbon fiber unidirectional layers. Composites: Part B 42 (2011) 1578–1587

[30] Karhunen K, Seppänen A, Lehikoinen A, Monteiro P, Kaipio J. Electrical Resistance Tomography imaging of concrete. Cement and Concrete Research 2010;40:137–145.

[31] Polydorides N, Lionheart W. A Matlab toolkit for three-dimensional electrical impedance tomography: a contribution to the Electrical Impedance and Diffuse Optical Reconstruction Software project. Meas Sci Technol 2002;13:1871–1883.

[32] Zhang W, Sakalkar V, Koratkar N. In situ health monitoring and repair in composites using carbon nanotube additives. Appl Phys Lett 2007;91(13):1–3.

[33] Kaupinnen P, Hyttinen J and Malmivuo J. Sensitivity distribution visualizations of impedance tomography measurement strategies. Int J Bioelectromagn 2006; 8(1): VII/1–9.

[34] Ali Naghashpour, Suong Van Hoa, "A technique for real-time detecting, locating, and quantifying damage in large polymer composite structures made of carbon fibers and carbon nanotube networks", Structural Health Monitoring, IN PRESS, doi: 10.1177/1475921714546063

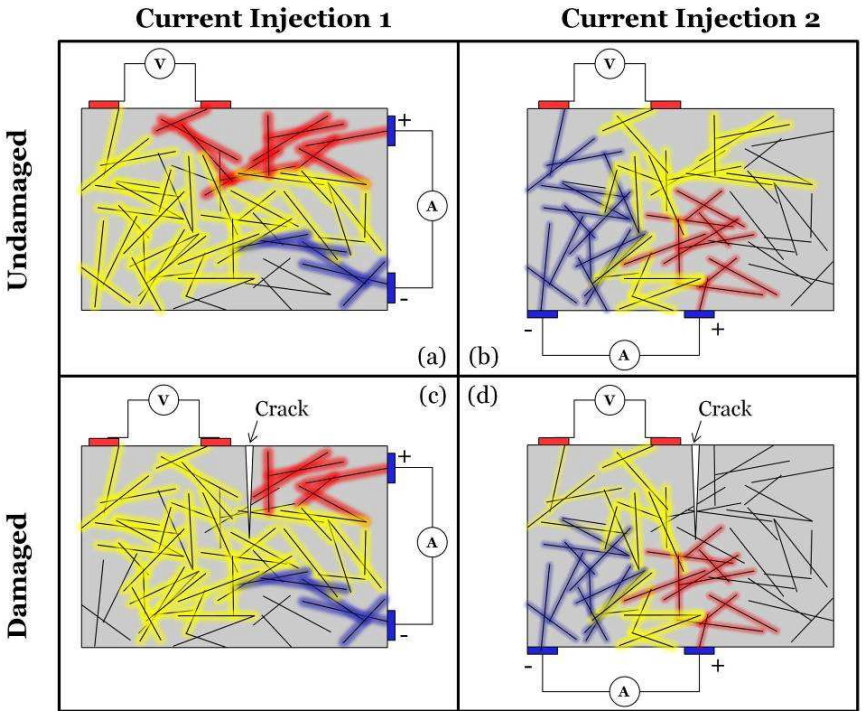

Figure 1. CNT network exploitation and Principle of ERT technique; (a), (b) undamaged material, (c), (d) damaged material. (Red: High voltage, Yellow: Medium voltage, Blue: Low voltage).

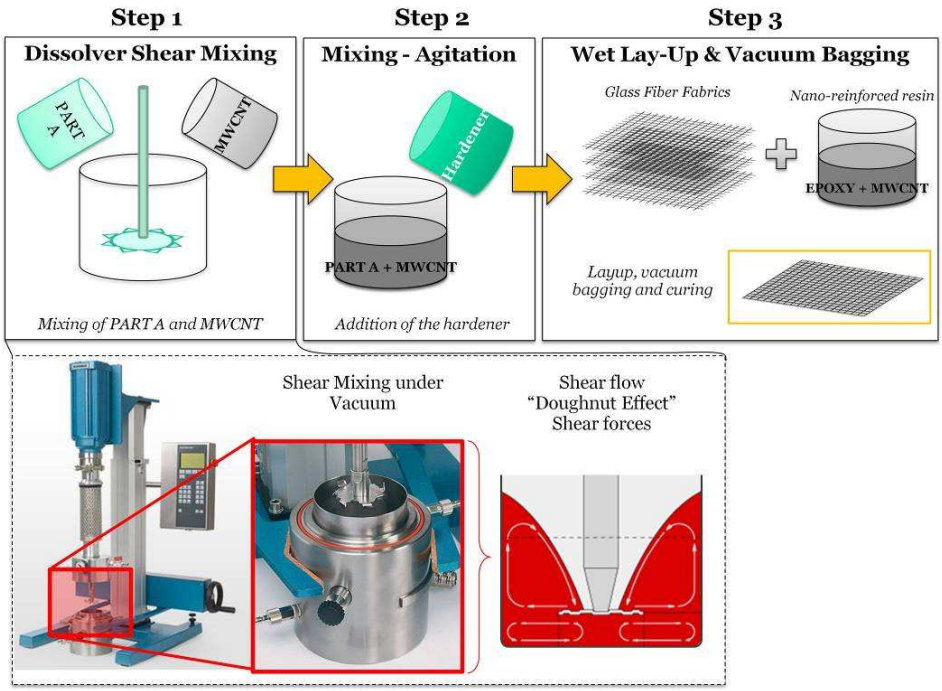

Figure 2. Preparation steps for producing a CNT reinforced polymer and GFRP plates with integrated CNT network.

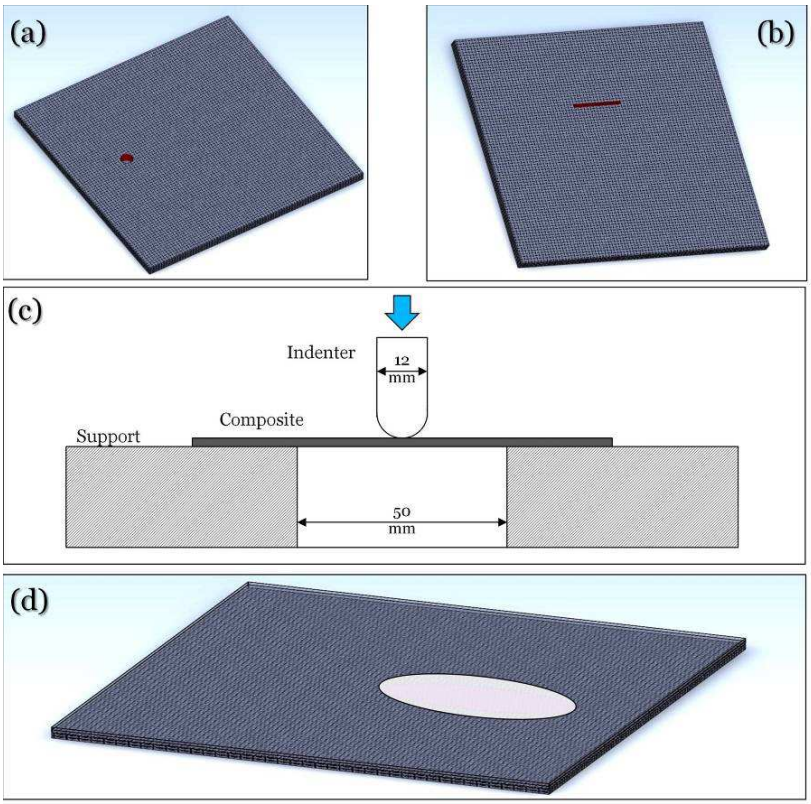

Figure 3. Investigated damage modes for composites: (a) drilled through-hole, (b) through-thickness notch, (c) Quasi-Static Indentation setup employed, (d) QSI induced interlaminar damage (in-plane).

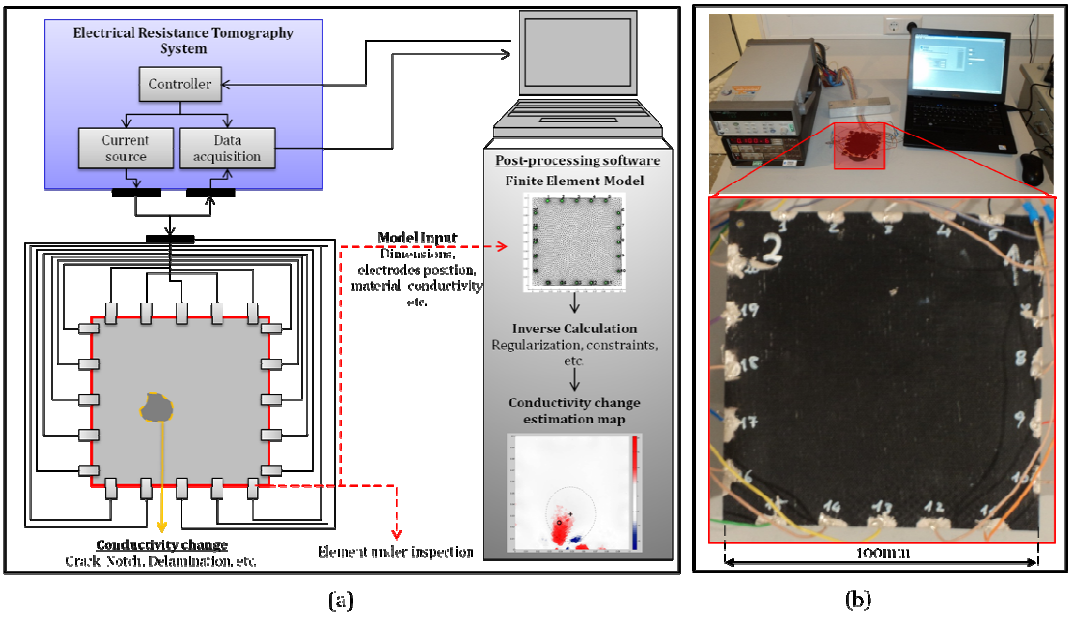

Figure 4 – Electrical Resistance Tomography System: (a) Conceptual diagram of the part, the ERT system and the processing unit, (b) Developed ERT setup and tested specimen.

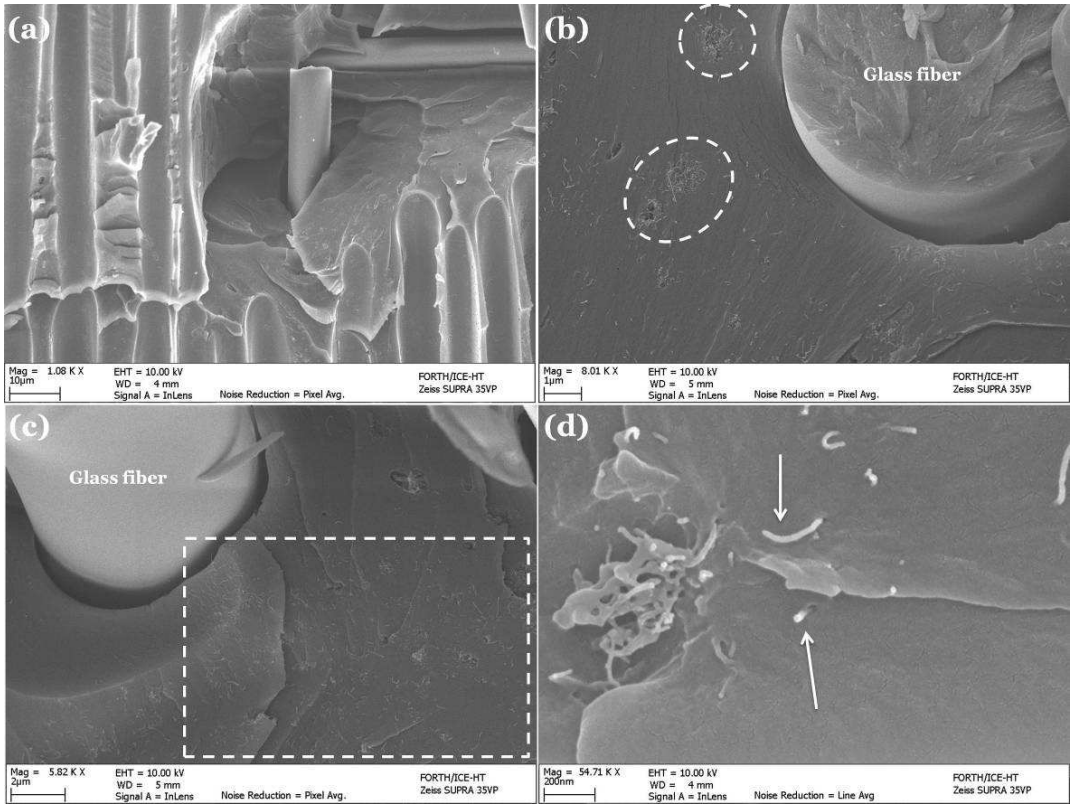

Figure 5. CNT network inspection using SEM micrographs at different magnifications: (a) Overview of CNT-GFRP fracture surface, (b), (c) Dispersion of CNT in the interfiber region, (d) Close-up of broken CNT agglomerate and free standing CNT. (scale-bar: (a)10μm, (b) 1μm, (c) 2μm, (d) 200nm)

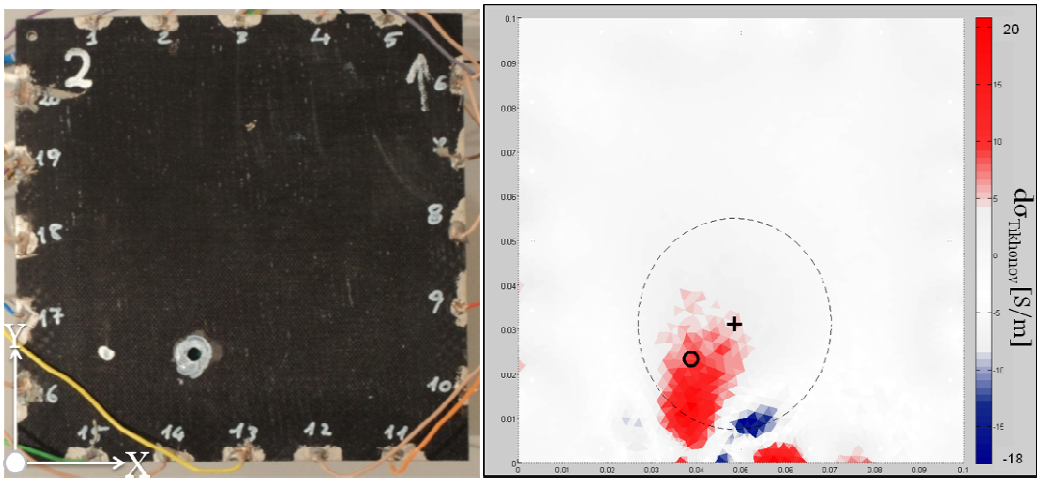

Figure 6. Through-hole damage: (a) Damaged specimen, (b) Reconstructed conductivity change map, where red indicates decrease in conductivity; Circle (o) indicates the real damage location, Cross (+) indicates the Centre of Interest, Dashed Ellipse indicates the Region of Interest.

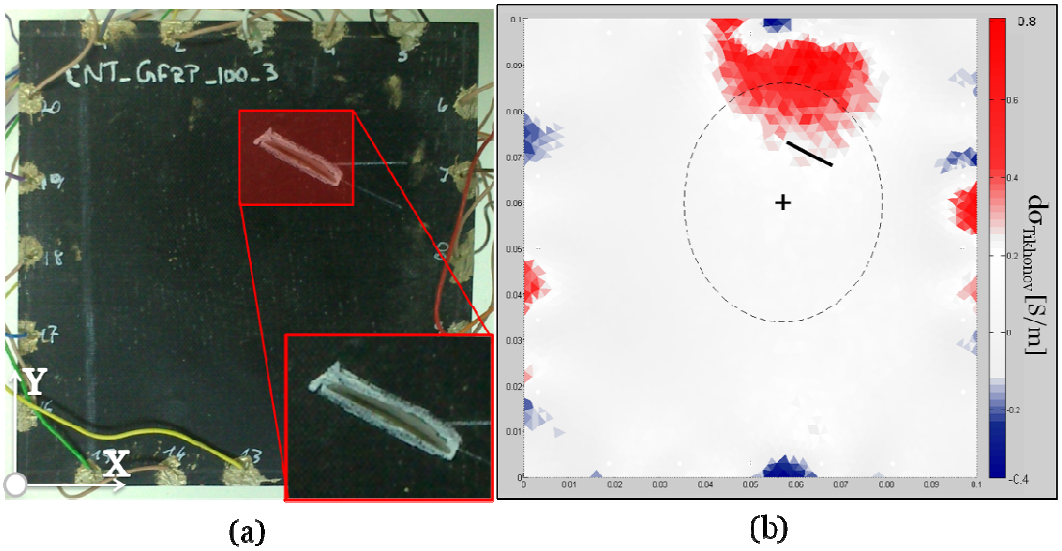

Figure 7. Oblong notch: (a) Damaged specimen, (b) Reconstructed conductivity change map, where red indicates decrease in conductivity; Line indicates the real damage location, Cross (+) indicates the Centre of Interest, Dashed Ellipse indicates the Region of Interest.

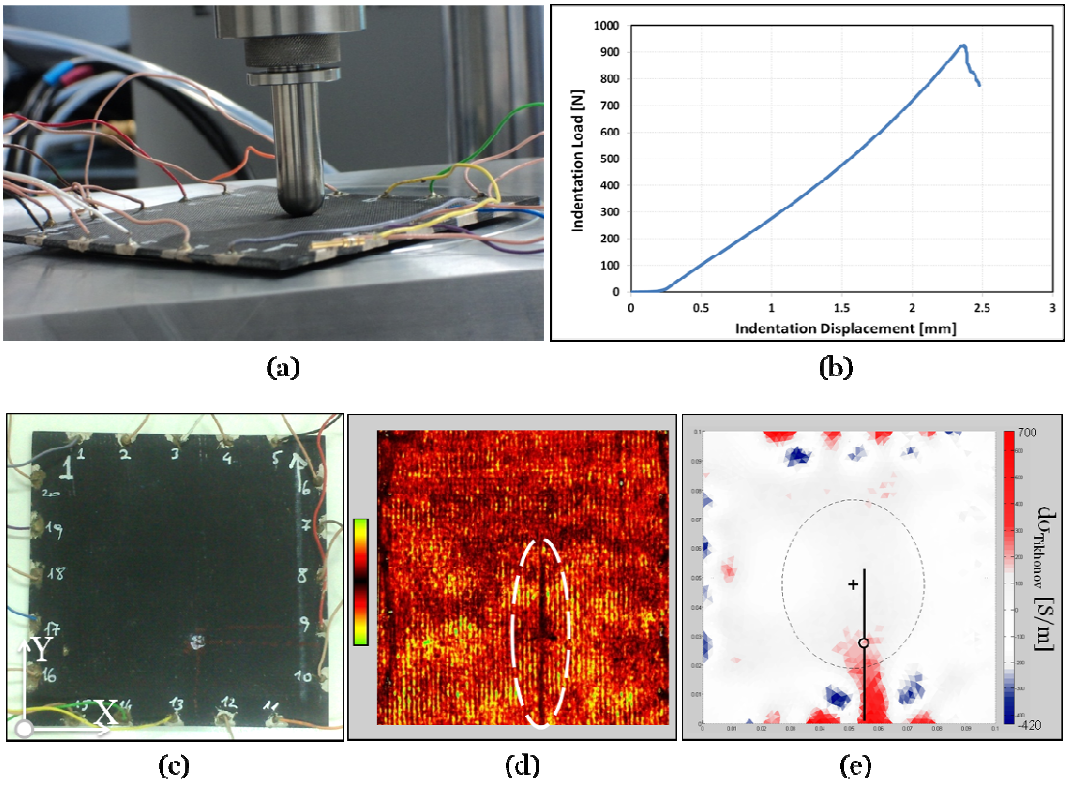

Figure 8. Interlaminar damage: (a) snapshot of the indentation experiment, (b) Force displacement diagram recorded for the CNT-GFRP. (c) Damaged specimen (d) Ultrasonic C-scan map: differentiation in color indicates different ultrasonic transmission and inhomogeneous structure, (e) Reconstructed conductivity change map, where red indicates decrease in conductivity; Circle (o) and continuous lines indicates the real damage location and extend, Cross (+) indicates the Centre of Interest, Dashed Ellipse indicates the Region of Interest.